Journal of Medical Devices Technology
jmeditec.utm.my

Original Research

STUDY OF LOCKING COMPRESSION PLATE THROUGH BIODEGRADABLE IMPLANT

Muhammad Syawal Aiman Sulong[1], Ardiyansyah Syahrom[1,2], Zulfadzli Zakaria[2*]

[1] *Department of Applied Mechanics and Design, Faculty of Mechanical Engineering, Universiti Teknologi Malaysia, 81310 UTM Johor Bahru, Johor, Malaysia*
[2] *Medical Devices and Technology Centre, Institute of Human Centered Engineering, Universiti Teknologi Malaysia, 81310 UTM Johor Bahru, Johor, Malaysia*

ARTICLE INFO

Article History:
Received 29 September 2022
Accepted 1 October 2022
Available online 3 October 2022

Keywords:
Implant,
Degradable Implant,
Compression Plate,
Plate and Screw,
Magnesium.

ABSTRACT

Orthopaedic implant biomechanics research is booming, especially in bone fixation. Fixation involves securing a plate to a broken bone. The femur fractured mostly. Long bone fractures can be difficult to cure despite technological and medical breakthroughs. This study analyses the performance and optimal screw arrangement for biodegradable locking compression plate. This study compares biodegradable bone plate materials to identify the best (Iron, Zinc and Magnesium). SolidWorks models fracture repair plates and fixes them in a normal walking condition to a mid-ship fracture. Further, finite element analysis was performed on models with homogeneous and isotropic bone and plate. Simulation was done using COMSOL programme and screws. Idealized poroelastic 3D FE femoral model with 5 mm fracture gap and plate-screw design. We saw stress and displacement. The minimal von Mises stress and deformation for 6 screws. Under pure zinc and magnesium load, the highest von Mises stress was 7.94 MPa and the maximum deformation was 0.08 mm, proving that iron was the best material. Based on finite element analysis, the LCP can offer mechanical stability for comminuted fractures, fixing the bone block and promoting bone healing.

INTRODUCTION

Implants and other medical devices have been developed specifically for complicated fractures. Traditional treatments for open fractures have been phased out in favour of more modern methods that accelerate secondary wound healing. Surgery and enhanced fixation devices are used to treat elderly patients in an effort to increase their mobility. When a bone is broken, an orthopaedic surgeon will merely realign the fractured bones and wait for them to heal before moving on to the next patient. As long as the surgeon correctly aligns the fractures and implants them, the patient has no responsibility in the establishment of a union (Rahim et.al, 2018; Böstman, 1994)).

Implant misposition can cause malunion as well as non-union, which ultimately results in a loss of function. Reduced risk of morbidity and mortality associated with subsequent operations The AO group has created novel implants for the treatment of multiple types of fractures, such as shaft fractures in adults, which are treated with dynamic compression plates. Plate screws are kept securely in place on plate threads by locking compression plates (Reichert et al, 2011). In order for the system to be finished, the plate and the screw need to be combined. In this situation, backing out of the screw can prevent the screw from failing, which would also prevent the plate from becoming loose and would prevent the fixation from failing. It provides a wide variety of alternatives for securing, and research has shown that it is helpful for both bone fragments and replacements (Mittal et.al, 2004). The preceding study, the objective of which was to develop a locking compression plate temporary implant for the following generation, served as the basis for this (Patel, 2006).

* Zulfadzli Zakaria
Medical Devices and Technology Centre, Institute of Human Centered Engineering, Universiti Teknologi Malaysia, 81310 UTM Johor Bahru, Johor, Malaysia.

MATERIALS AND METHOD

Design of Locking Compression Plate

The model of the screw-plate fixation system was designed and developed using the computer-aided design (CAD) software SolidWorks. The LCP's dimensions are as follows, the length of the plate is 186 mm, the width of the plate is 16 mm, and the thickness of the plate is 5 mm as seen in Figure 1. The slots on the plate were formed by using two-hole wizard magic on the plate. Hole wizard sketches are exhibited. The actual plate was utilised to measure out 18 millimetres as the precise linear distance that was employed in the creation of the design. The extrude cut feature and a circle with a diameter of 2.5 mm were used to create each and every one of the groove patterns that are seen in the image that can be found below. The linear pattern is located 18 mm away, as can be seen in Figure 2 (Rokkanen et al, 2000)

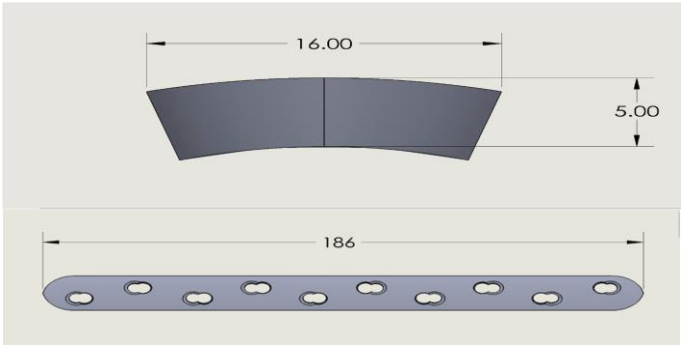

Fig. 1 Side view shows the convex curvature of the plate, with an extrude boss or base situated at 186mm.

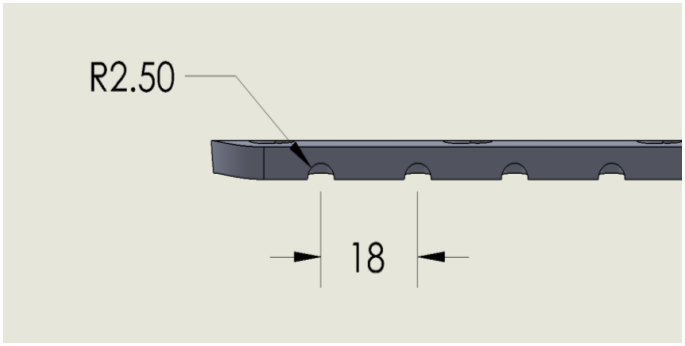

Fig. 2 Linear pattern of the grooves.

Design of screw

Bolts come in a variety of lengths, each of which has a standard diameter of 5 mm and can be utilised in a manner that is appropriate for the size of the gap that is being connected. The length of each of the bolts in the design is 20 mm. The design was constructed using the actual bolt as a source of measurement information. Please refer to Figure 3 in order to view a sketch of the profile of the bolt where the major diameter, d1 = 8.0 mm, the minor diameter, d2 = 5.0 mm and the over length, L= 20.0 mm (Huiskes et.al, 1992).

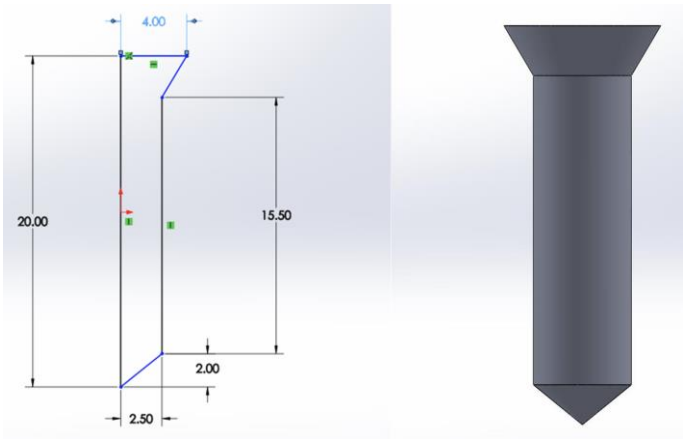

Fig. 3 Sketch of bolt cross section and model of locking screw.

Establishment of a Finite Element Model for Femoral Fixation Femoral Fixation Geometrical Model

A geometrical method is utilised in the modelling process of the non-displaced femoral in the SolidWorks software. The bone fracture gap was set at a constant of 5 mm. In the previous research, the femur bone was broken in half for examination purposes. In Figure 4a, the bone was cut at a 45-degree angle. As shown in Figure 4b, the fragmented bone was set to 5 mm in the z-axis direction. This was done so that the non-displaced femoral condition could be established (Juutilainen et.al, 1997).

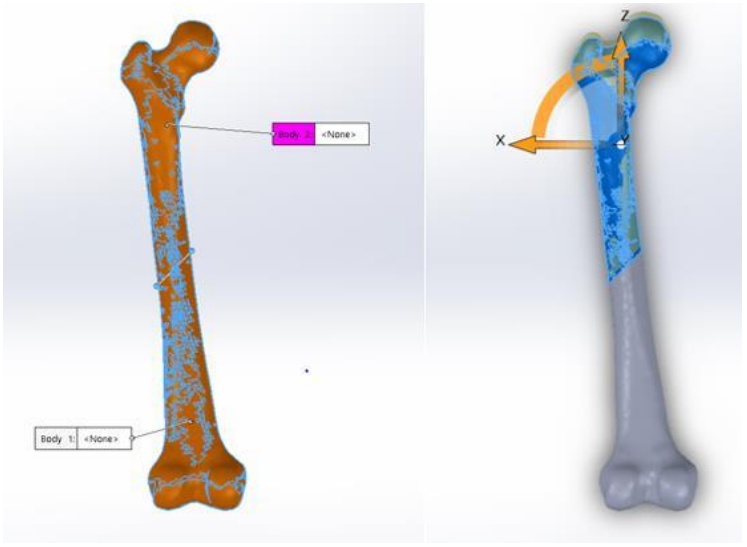

Fig. 4 a) Split at 45-degree plane. b) Fracture gap of 5 mm on z direction.

The bone plate and fractured femur bone in the SolidWorks program are created by using the tools in the software that are respectively named bone plate and broken femur bone. The LCP was pieced together so that the bone structure and bone fragments would be compatible with one another. An up-angled screw was used to heal the break in the bone, and a screwed plate was used to reunite the broken pieces of bone. This procedure was modelled in SolidWorks (Puleo and Nanci, 1999).

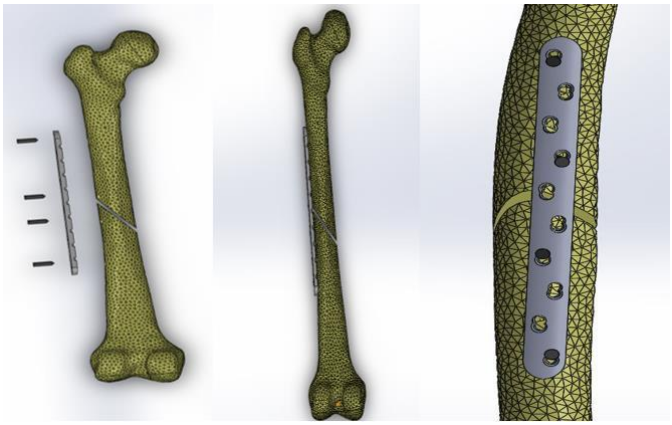

Fig. 5 Exploded view and three-dimensional views of assembled model.

The holes in the middle of the plate are considered to be empty since they are required for the correct distribution of the weight via the screws and plate. It's possible to penetrate the side of the bone if you use screws that are too lengthy. Plates are secured to the tensile curve of the femur bone in order to counteract the effect of the bone's tensile surface searching for compressive stresses to balance the stresses. Alternately securing the screws to the plate and bone is also conceivable, which helps to relieve stress that is caused by the pre-tightening process. During the process of assembly, you should take precautions to ensure that the stress is applied to the screws and not the plate (Zare et.al, 2014). The sole purpose of installing the plate is to provide support for the femur bone. This ensures that the femoral bone is subjected to the least amount of stress possible (Wegener et.al, 2011).

COMSOL added the fixation systems fixation systems into the software so that it could more accurately simulate the process of constructing femoral fracture models and fixation systems. The file was produced using the SolidWorks application, and it was saved using the SolidWorks Assembly file format. Through the use of Live Link, geometry may be transferred from SolidWorks to COMSOL. To synchronise your devices, select the "synchronise" option. The analysis can begin once the model has been prepared for it and is ready to go. The imported geometry may be seen in Figure 6 of the COMSOL file .

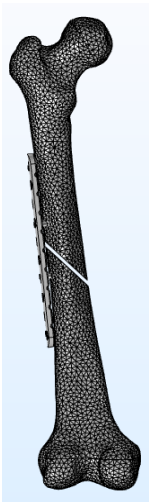

Fig. 6 Geometry of assembled view in COMSOL software.

After the development of a model, the surface mesh for the femur bone model that will be used in subsequent iterations of the finite element analysis is produced (FEA). When requesting extra fine mesh, it is imperative that you provide the required mesh size. There were a total of 522747 elements created. The meshed model of the femur bone that was created in COMSOL may be shown in Figure 7. A complete mesh would be an example of a mesh that contains 522747 domain elements, 81835 triangle elements, 30504 edge elements, and 4460 vertex elements.

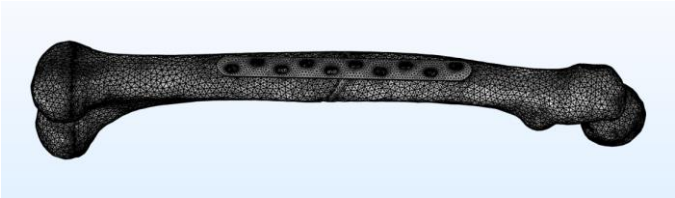

Fig. 7 Meshing geometry

Computations involving structures use a FEA mesh to represent the nodes and elements of the structure. In the course of working on this project, a 3D CAD model of a femur bone was utilised in order to construct a FEA mesh. The meshes used for the Finite Element Analysis were constructed using free tetrahedral 1 elements. The aforementioned element type was chosen because of the superior precision it possesses in comparison to its less powerful counterpart. The FEA mesh was constructed with the help of the auto-mesh creation method found in the FEA software COMSOL. By doing mesh refinement in chosen bone segments instead, we were able to avoid the sites of stress concentrations. In addition, adjustments were made to the mesh in areas with steeper gradients in order to improve the accuracy of the results. In addition to that, a sensitivity analysis of the mesh was carried out to ensure the accuracy of the results. Figure 7 depicts the FEA mesh used to analyse the femur bone (Ramadhoni et.al, 2020).

Mesh convergence studies were carried out in order to determine which mesh resolutions are best suited for different regions of the model. The results of these studies revealed that the mesh resolutions that had the greatest impact on the highest Von Mises stress (VMS) on the plate were the ones that were best suited for this purpose.

The limitations and problems that were discovered throughout the course of this research were incorporated into the activities that patients often engage in after undergoing total hip replacement. Simulations with a vertical load while the subject is walking normally in most cases. The loading cycle will become visible once all of the normal walking circumstances have been exhibited.

Axial compression was applied to the head region of the femur, which produced an effect that was analogous to the weight that is exerted on the head of the femur when the body is in the typical upright position. Because the weight of an adult person, which is determined by selecting the face area that is displayed in Figure 8a, is very close to the define weight at the femur head in the downward direction, we estimate that the maximum gait load in the current situation is 2000 N, and it acts in the downward z-direction. This conclusion is based on the information that is discussed in Ramadhoni et al. (2020), and it acts in the downward z-direction.

Support is added to the tibia or lower end of the femur bone by selecting the bottom end of the femur bone in Figure 8b. This creates a more stable structure. The state of the thing being fixed and confined in all three dimensions is what the noun "rigid" refers to. The object has a free end at the top, also known as the head.

Because the material properties of the human femur vary greatly between individuals, it is difficult to ascribe exact material features. The bone was considered isotropic while being anisotropic. However, the analysis of the complete femur bone was employed to compute the in-plane and out-of-plane bone material distribution. Due to the fact that it is possible to partially solve for an anisotropic solution, the argument is that a little quantity of bone can be obtained with it. For a whole bone, however, the assignment of anisotropic material properties is significantly more challenging. The mechanical properties of biomaterial for femur, plate and screw as shown in Table 1. The modulus of the femur bone of young females can range between 10 and 20 GPa. Analysis revealed that the modulus was 18.6 GPa. The Poisson ratio and density employed were 0.3 and 2,000 kg/m3, respectively. This experiment utilised a linear elastic material model. When performing a linear static analysis, physiological conditions (muscle involvement in load distribution) were disregarded (Yin et.al, 2018).

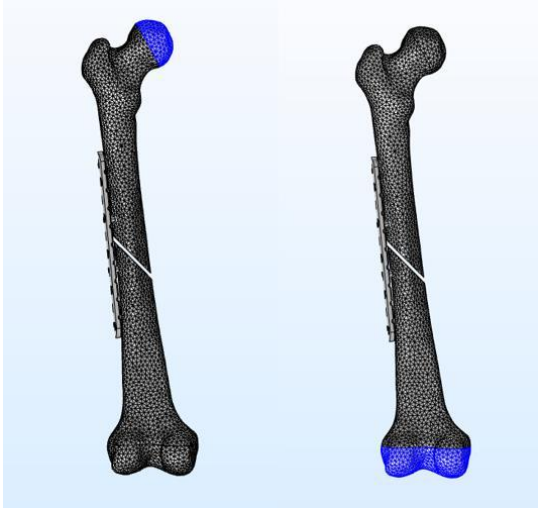

Fig. 8 (a) Load at the head surface of femur. (b) Fixed support in the lower surface.

The models were uploaded to COMSOL, where finite element analysis was utilised to confirm the models finite dimensionality. After assembling the femur, the LCP and screws were checked. Each simulation was conducted on a metal container made entirely of biodegradable materials. The analysed research boundaries were identical to those of the uniaxial compression experiments. The distal end of the femur was restrained from movement and rotation, allowing it to keep its normal position. A vertical point load of 2000 N was applied to the most superior node on the femoral head, which represents the maximum gait load for a normal walking cycle. This is the patient's weight, hence the force exerted on the LCP is dependent on it. While analogous study has been conducted to analyse the stress, concentration factors of the screw holes, and shear stress on the screws, this investigation has proven that the stress concentration factors of the screw holes and shear stress on the screws lead to equivalent outcomes. Stress was applied to the screw to determine whether or not the stresses at the screw-bone contact are crucial for the LCP's stability. Due to the forces involved in standard plating designs, particularly in the absence of bone contact to transfer the stress, the risk of screw failure during loading is clinically significant (Oriňák et al, 2014).

Table 3 Mechanical properties of biomaterial for femur, plate and screw.

Bone and Material	Density, ρ (kg/m^3)	Young's Modulus, E (GPa)	Poisson Ratio, v
Femur bone	2000	18.6	0.3
Iron	7870	200	0.29
Zinc	7100	90	0.25
Magnesium	1730	44	0.28

This procedure sets the values of three variables. In the initial step, all geometric models were converted to free tetrahedral geometry. In addition, it was assumed that the model material properties, such as isotropy, homogeneity, and linear elasticity, were consistent throughout the model domain. This study will explore the consequences of different implant material qualities; hence, three sets of full models with similar material attributes, excluding implant materials, have been developed (Tan et.al, 2013).

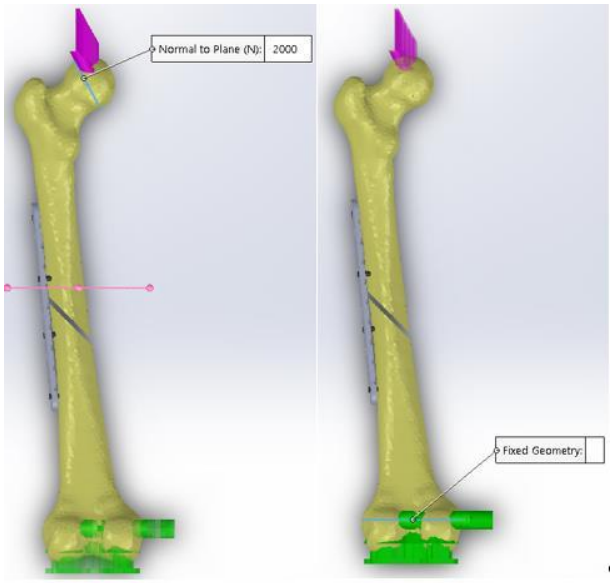

Fig. 9 (a) Load at the head surface of femur. (b) Fixed support in the lower surface.

In addition, two sets of boundary conditions were assigned to the entire model. At each node, the fixed boundary was bounded by the bottom model. As shown in Figure 9, the second group utilised a weight of 2000 N on the femoral head.
The analysis's output results were decided by two parameters. It is identical to von Mises' assertion regarding implant stability, which states, "The first is all-important in terms of implant stability." To analyse the mobility of the implant, you must provide the second parameter, which is displacement. When selecting the implant mobility that will result in the most stable and acceptable joint function, the most stable and adequate joint mobility is always chosen (Zheng et.al, 2014).

RESULT AND DISCUSSION

Stress behaviour of different screw placement and number of screws

Von Mises stress is a geometric combination of the stresses acting in all three spatial dimensions (x, y, and z) and moreover in only one of those directions (usually along the third dimension). Von Mises' yielding prediction method is useful for forecasting when materials are likely to yield after being loaded.

The applied stress values in this experiment were based on the von Mises stress value with the highest value (Liu et al, 2015).

The number and location of screws used for a certain application can be altered. In order to distribute the load evenly, the quantity and location of screws must be carefully considered. Reducing the number of screws reduces the overall load, allowing for greater load concentration on each individual screw. This concept was explored by varying the number and positioning of screws in the present study (Jurgeleit, 2015).

Four screws were utilised in the preliminary analysis, whereas eight screws were utilised in the final judgement. Two screws on the plate were left empty to prevent the fracture from worsening. Four screws were necessary to support the plate, two at each end. In order to prevent the plate from moving from its precise spot, it must be impossible to remove. In this way, it becomes an even better plate to hold the fragmented bone and provide the most support possible. Before tightening the remaining screws, the two closest to the fracture line must be screwed in. If two of the three screws closest to the fracture line are tightened during surgery, the doctors will not need to order the other screws (Yin et.al, 2018).

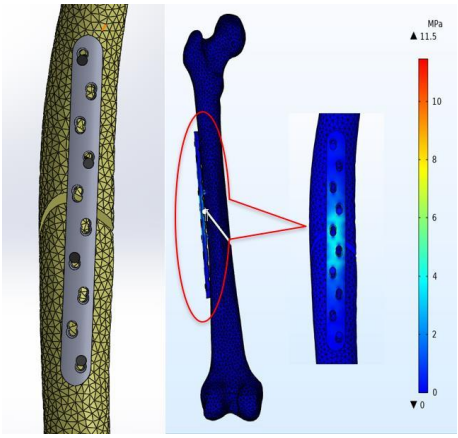

Fig. 10 The contour plots of von Mises stress of the femur for 4 screws.

The contour plots of von Mises' stresses on the femur for four screws are illustrated in Figure 10. During normal walking, the contact between the screw and bone exhibited significant stress concentration. Regarding von Mises' theory, we can observe that his stress has the highest value of 11,05 MPa. As demonstrated by the colour range contour map, the middle of the plate had the greatest amount of stress. Plate's two screw holes were surrounded by an increasing level of stress. Due to the small level of stress elsewhere on the bone, it is only possible to detect strain on the implant (Zheng et.al, 2014).

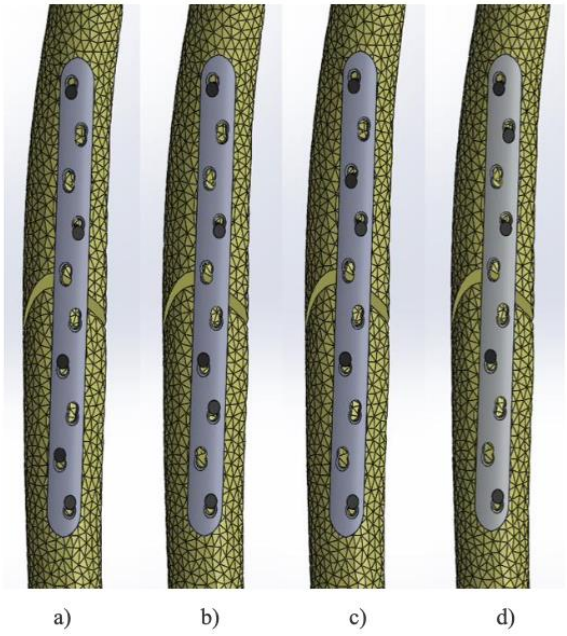

Fig. 11 Four different types of screw arrangement using 5 screws (a) screw arrangement 1 (b) screw arrangement 2 (c) screw arrangement 3 (d) screw arrangement 4.

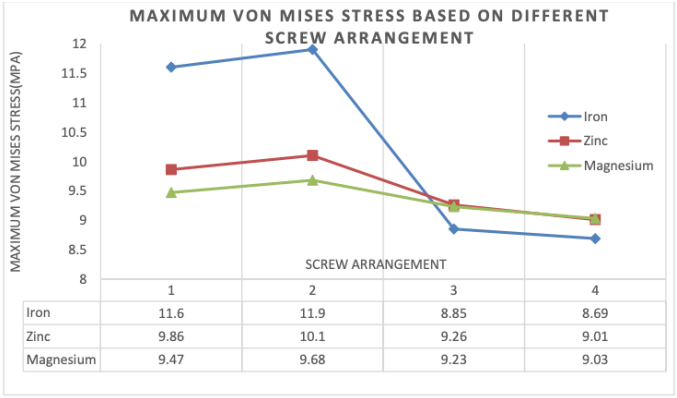

	1	2	3	4
Iron	11.6	11.9	8.85	8.69
Zinc	9.86	10.1	9.26	9.01
Magnesium	9.47	9.68	9.23	9.03

Fig. 12 The graphs representing maximum values of von Mises stress at the bone using four orientations of 5 screw with different implant material.

Based on Figures 11 and 12, it depicts the stress behaviour of the bone as a result of different screw placement and materials. When screw 4 is loaded with a force of 2000 N, von Mises stress values range from 8.69 to 9.03 MPa. Iron is the softest and least von Mises-stressed metal (8.69 MPa). The Von Mises stress value for screw 2 (11.9 MPa) was the highest, while the Von Mises stress value for screw 4 (8.69 MPa) was the lowest (Oriňák et al, 2014).

Fig. 13 Six different types of screw arrangement using 6 screws (a) screw arrangement 1 (b) screw arrangement 2 (c) screw arrangement 3 (d) screw arrangement 4 (e)screw arrangement 5 (f) screw arrangement 6.

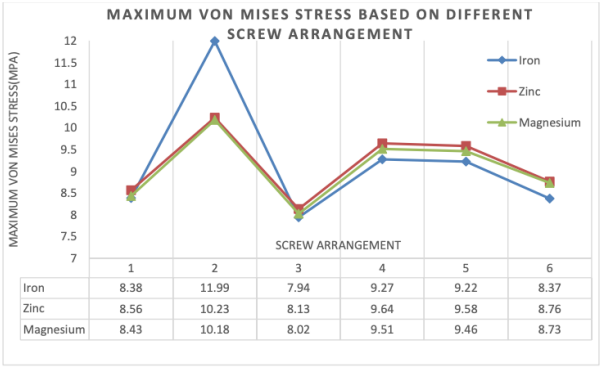

	1	2	3	4	5	6
Iron	8.38	11.99	7.94	9.27	9.22	8.37
Zinc	8.56	10.23	8.13	9.64	9.58	8.76
Magnesium	8.43	10.18	8.02	9.51	9.46	8.73

Fig. 14 The graphs representing maximum values of von Mises stress at the bone using four orientations of 5 screw with different implant material.

As seen in Figures 13 and 14, the stress exerted on the bone might vary depending on the screw and substance used. When screw 3 was set with its 7.94 MPa to 8.02 MPa value, a reasonable stress range of 7.94 MPa to 8.02 MPa was discovered. Von Mises' hypothesis accounts for the lowest stress in iron (7.94 MPa). The Iron material of screw 2 had the highest von mises stress at 11.99 MPa, while the Iron material of screw 3 had the lowest von mises stress at 7.94 MPa (Yin et.al, 2018).

Fig. 15 Four different types of screw arrangement using 7 screws (a) screw arrangement 1 (b) screw arrangement 2 (c) screw arrangement 3 (d) screw arrangement 4.

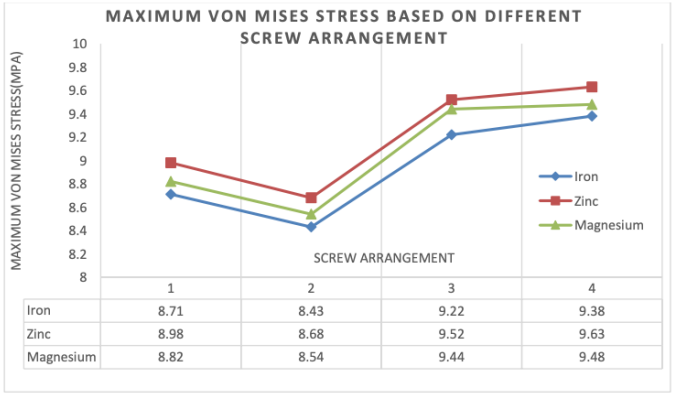

	1	2	3	4
Iron	8.71	8.43	9.22	9.38
Zinc	8.98	8.68	9.52	9.63
Magnesium	8.82	8.54	9.44	9.48

Fig. 16 The graphs representing maximum values of von Mises stress at the bone using four orientations of 7 screw with different implant material.

Based on Figures 15 and 16, the best stress for screw 2 configuration was between 8.43 and 8.54 MPa. Materials such as zinc (for the arrangement of screw 4) and iron (for the arrangement of screw 2) exhibited the highest von Mises stress values, with 9.63 MPa for zinc and 8.2 MPa for iron, respectively.

Fig. 17 Five different number of screw arrangement (a) 4 screws (b) 5 screws (c) 6 screws (d) 7 screws (e) 8 screws.

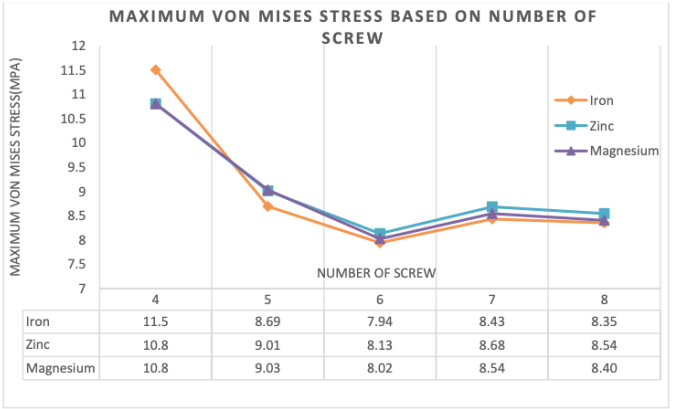

	4	5	6	7	8
Iron	11.5	8.69	7.94	8.43	8.35
Zinc	10.8	9.01	8.13	8.68	8.54
Magnesium	10.8	9.03	8.02	8.54	8.40

Fig. 18 Five different number of screw arrangement (a) 4 screws (b) 5 screws (c) 6 screws (d) 7 screws (e) 8 screws.

Based on Figures 17 and 18, these graphs depict the maximum von Mises stress values for the femur while securing the Locking Compression Plate with varying numbers of screws. The lowest von Mises stress rating is displayed next to the six screws. The material number of screws exhibits the lowest von Mises stress of 7.94 MPa among fasteners. Figure 18 demonstrates that the strains exerted on implants are less than the bone's ultimate strength (130 MPa), indicating that varying screw counts in implant constructions represent no additional risk to patients who are not at risk for a secondary fracture in the femur bone. If the bone's stress values are more than its ultimate strength, the medical team must implement safety steps to prevent secondary fractures (Zare et.al, 2014).

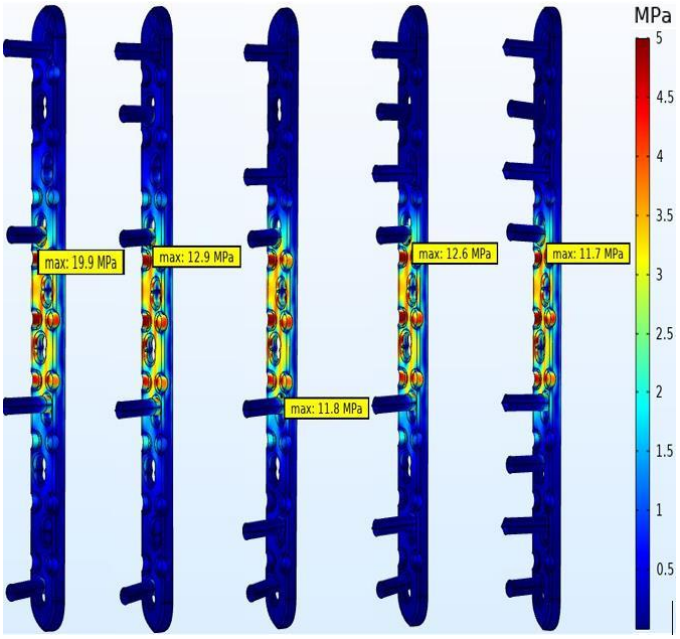

Fig. 19 Five different number of screw arrangement (a) 4 screws (b) 5 screws (c) 6 screws (d) 7 screws (e) 8 screws.

The stress levels measured in the implant and surrounding bone are depicted on a 0 to 5 MPa scale in Figure 19. Figure 19 illustrates the distribution of stress, which the table indicates is dependent on the number of screws. Considering all positions, the implant's centre was the location with the most stress. In general, stress levels were greater at the screw than at the plate. A four number of screws stress value (19.9 MPa) exceeds an eight number of screws stress value (8.2 MPa) (11.7 MPa) (Yin et.al, 2018).

The number of deformations or displacements that occur at the fracture site can be used to determine the stability of a fracture. It should be noted that a large displacement at the fracture bone can result in an unstable treatment construct during full weight bearing (Yin et.al, 2018). This experiment compared three distinct substances to see which substance induced the greatest amount of displacement. As shown in Figure 20, iron with a dimension of 0.08 mm created the optimal implant displacement (Liu et al, 2015).

Figure 21 shows that the pattern and amplitude of displacement induced by an iron implant were less than those induced by zinc or magnesium implants. In addition, the data demonstrate that magnesium implants result in significant implant displacement, indicating that the implant may have been distorted or twisted due to the relatively low modulus of magnesium compared to the other two metals, and may not be clinically acceptable. We can also notice that the value between screw numbers for these three materials is pretty similar (Oriňák et al, 2014).

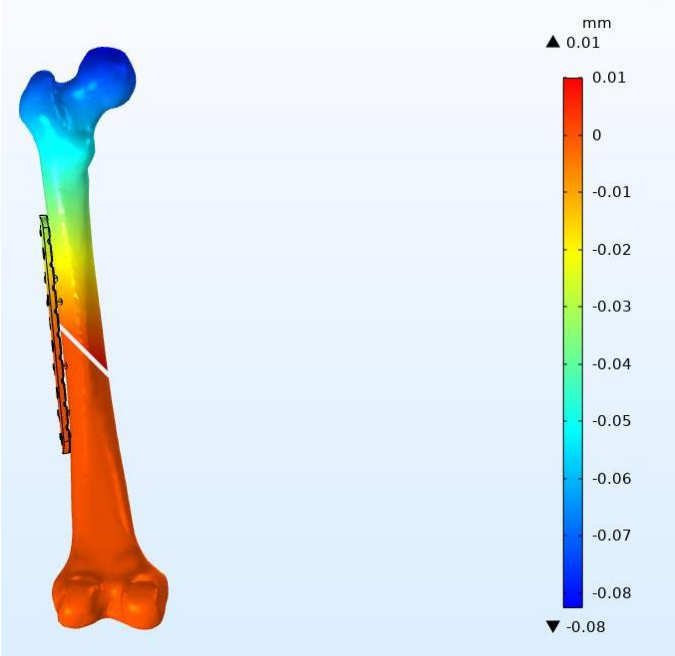

Fig. 20 The displacement of 6 screw for arrangement 3 along x direction.

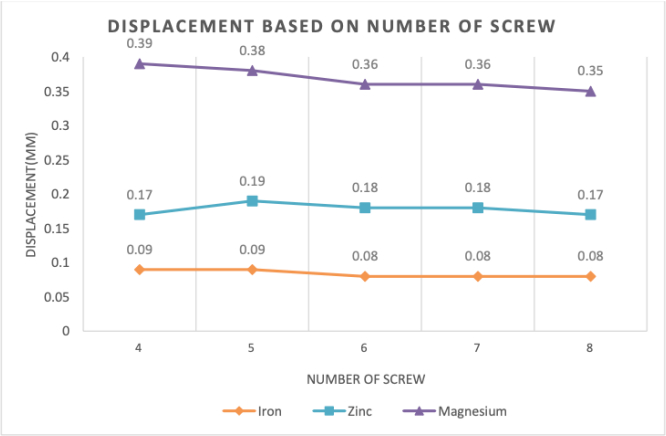

Fig. 21 Displacement behaviour on model components using iron, zinc and magnesium.

CONCLUSION

In this work, all three materials were effectively simulated in order to compare the stability of stress distribution in LCP in order to study the effectiveness bone treatment options. According to the data, implant stress was greater than femur bone stress. It was discovered that the optimal 6 screws for arrangement 3 have a value of 7.94 MPa and a yield strength value below 50 MPa, indicating that iron is the best suitable implant material. With fewer screws, there was minimal disruption to the blood flow and an optimal mechanical environment for tissue differentiation. Additionally, a temporary increase in stress within the implant as a result of the presence of four screws could lead to a reduction in stress shielding and osteoporosis. Actually, all of the materials can be employed because they do not achieve Yield's strength, but simulations indicate that Iron performs better than Zinc and Magnesium. In

terms of stress on implant, eight screws 11.7 MPa exhibit the lowest stress, although only by 0.1 MPa when compared to six screws 11.8 MPa. The screw must be robust and flexible in order to stabilise the fractured bone, but its strength should not surpass that of the bone itself. If the value exceeds the yield strength, the material will bend plastically and break; therefore, this situation should be avoided. This research demonstrates that the screws are safe for femur because they are neither distorted or fractured. Iron has the lowest stability in terms of displacement compared to the other two materials. The stability of LCP is dependent on the number of screws on the plate, therefore reducing the number of screws will lessen the implant's stress distribution. Due to the low force required to create bone contact, this is the case. Reduce the bone resorption process, which will weaken the bone structure, by minimising the shielding effect. Fe exhibits the least displacement in dx and dz direction compared to Zn and Mg. In the dy direction, however, Fe exhibits the greatest displacement relative to Zn and Mg. In general, the displacement values for all plates were below 1 mm, but Fe exhibited the lowest displacement. Thus, Fe is the most suited implant material. The use of a suitable number of anchoring screws to press the plate against the bone with substantial compressive stresses, so generating a stable bone-implant connection, is the foundation of conventional plating techniques. Combining two distinct anchorage systems in a single implant is the innovative and revolutionary component of the LCP. The significance of the reduction approach and minimally intrusive plate insertion and fixation lies in their ability to preserve bone vitality. This plate is likewise put directly to the bone surface, therefore the shielding force must be kept to a minimum. To reduce the bone resorption process, which will degrade bone structure, it is necessary to minimise the shielding effect.

ACKNOWLEDGEMENT

This study was sponsored Medical Devices and Technology Centre, Institute of Human Centered Engineering, Universiti Teknologi Malaysia.

REFERENCES

Böstman O. 1994. Economic Considerations on Avoiding Implant Removals after Fracture Fixation by Using Absorbable Devices. Scand. J. Public Health 22(1), 1–45.

Huiskes R., Weinans H., and Van Rietbergen B. 1992. The relationship between stress shielding and bone resorption around total hip stems and the effects of flexible materials. Clin. Orthop. Relat. Res 274, 124–134.

Jurgeleit T., Quandt E., and Zamponi C. 2015. Magnetron sputtering a new fabrication method of iron based biodegradable implant materials. Adv. Mater. Sci. Eng 2015, 1-9.

Juutilainen T., Pätiälä H., Ruuskanen M., and Rokkanen P. 1997. Comparison of costs in ankle fractures treated with absorbable or metallic fixation devices. Arch. Orthop. Trauma Surg 116 (4), 204-208.

Li Z., Gu X., Lou S., and Zheng Y. 2008. The development of binary Mg-Ca alloys for use as biodegradable materials within bone. Biomaterials 29(10), 1329-1344.

Liu X., Sun J., Zhou F., Yang Y., Chang R., Qiu K., Pu Z., Li L., and Zheng Y. 2016. Micro-alloying with Mn in Zn-Mg alloy for future biodegradable metals application. Mater. Des. 94, 95-104.

Mittal R., Morley J., Dinopoulos H., Drakoulakis E. G., Vermani E., and Giannoudis P. V. 2005. Use of bio-resorbable implants for stabilisation of distal radius fractures: The United Kingdom patients' perspective. Injury 36(2), 333-338.

Oriňák A., Oriňáková R., Králová Z. O., Turoňová A. M., Kupková M., Hrubovčáková M., Radoňák J., and Džunda R. 2014. Sintered metallic foams for biodegradable bone replacement materials. J. Porous Mater 21,131-140.

Patel V. 2006. Biomechanical Evaluation of Locked and Non-locked Constructs Under Axial and Torsion Loading. Wright State University (Master Thesis).

Puleo D. A. and Nanci A. 1999. Understanding and controlling the bone-implant interface. Biomaterials 20 (23–24), 2311-2321.

Rahim M. I., Ullah S., Mueller P. P. 2018. Advances and challenges of biodegradable implant materials with a focus on magnesium-alloys and bacterial infections. Metals 8(7), 532.

Ramadhoni T. S., Syahrom A., Md Saad A. P., Prakoso A. T., Wicaksono D., and Basri H. 2020. The Analysis of Wear on Artificial Hip Joint with Dimple on Femoral Surface. J. Phys. Conf. Ser 1500(1), 1-8.

Reichert W. M., Ratner B. D., Anderson J., Coury A., Hoffman A. S., Laurencin C. T., and Tirrell D. 2011. 2010 Panel on the Biomaterials Grand Challenges. J. Biomed. Mater. Res. - Part A, 96 A (2), 275-287.

Rokkanen P. U., Böstman O., Hirvensalo E., Mäkelä E. A., Partio E. K., Pätiälä H., Vainionpää S. I., Vihtonen K., and Törmälä P. 2000. Bioabsorbable fixation in orthopaedic surgery and traumatology. Biomaterials 21(24), 2607-2613.

Tan L., Yu X., Wan P., and Yang K. 2013. Biodegradable Materials for Bone Repairs: A Review. J. Mater. Sci. Technol 29(6), 503-513.

Tie D., Guan R., Liu H., Cipriano A., Liu Y., Wang Q., Huang Y., and Hort N. 2016. An in vivo study on the metabolism and osteogenic activity of bioabsorbable Mg-1Sr alloy. Acta Biomater 29, 455-467.

Wegener B., Sievers B., Utzschneider S., Müller P., Jansson V., Rößler S., Nies B., Stephani G., Kieback B., and Quadbeck P. 2011. Microstructure, cytotoxicity and corrosion of powder-metallurgical iron alloys for biodegradable bone replacement materials. Mater. Sci. Eng. B Solid-State Mater. Adv. Technol. 176(20), 1789-1796.

Yin G. Z., Yang X. M., Zhou Z., and Li Q. F. 2018. A green pathway to adjust the mechanical properties and degradation rate of PCL by blending bio-sourced poly(glycerol-succinate) oligoesters. Mater. Chem. Front. 2(3), 544–553.

Zare E. N., Lakouraj M. M., and Mohseni M. 2014. Biodegradable polypyrrole/dextrin conductive nanocomposite: Synthesis, characterization, antioxidant and antibacterial activity. Synth. Met. 187(1), 9-16.

Zheng Y. F., Gu X. N., and Witte F. 2014. Biodegradable metals, Mater. Sci. Eng. R Reports 77, 1-34.